# Controlling the refractive index and third-order nonlinearity of polyimide/$Ta_2O_5$ nanolaminates for optical applications

Running title: Third-order nonlinearity of polyimide/$Ta_2O_5$ nanolaminates

Running Authors: Färm et al.

Elina Färm[1,2], Soroush Mehravar[3], Khanh Kieu[3], N. Peyghambarian[3], Mikko Ritala[1], Markku Leskelä[1], and Marianna Kemell[1,a)]

[1]Department of Chemistry, University of Helsinki, FI-00014 Helsinki, Finland

[2]Present address: ASM Microchemistry, Pietari Kalmin katu 3 F 2, FI-00560 Helsinki, Finland

[3]College of Optical Sciences, University of Arizona, Tucson, AZ 85721, USA

[a)] Electronic mail: marianna.kemell@helsinki.fi

In this study we investigated third-order optical nonlinearity in polyimide/$Ta_2O_5$ nanolaminates deposited by atomic layer deposition. Third harmonic signal measurements were done with a multiphoton microscope at excitation wavelength of 1.55 μm, laser pulse duration 150 fs and estimated pulse energy 1.2 nJ. Third-order optical nonlinearity is an essential property in optical signal applications for telecommunication. Transparency at telecommunication wavelengths as well as a high refractive index are desired for a material. Polyimide is optically transparent, enabling light guidance through the material. The refractive index of the material can be fine-tuned by combining polyimide with a substantially higher refractive index material – in this case $Ta_2O_5$. The layer thicknesses in nanolaminates were varied and the third harmonic generation was compared to plain polyimide and $Ta_2O_5$ reference films. Third harmonic generation in the nanolaminates decreased slightly and refractive index increased with increasing $Ta_2O_5$ content.

Normalized third-order nonlinear susceptibilities, $\chi^{(3)}$, calculated for the nanolaminates were between the values of $Ta_2O_5$ and polyimide and increased with increasing polyimide content.

# I. INTRODUCTION

Polyimide is an optically transparent material which makes it an interesting candidate for optical waveguide applications in telecommunication. In addition to optical transparency, also high third-order nonlinearity is needed for silicon nanophotonic devices[1,2,3]. Polyimides and polyisoimides with conjugated structures have also shown high third-order nonlinearities[4]. However, polyimide has a low refractive index (1.58 at 517 nm). Because third-order nonlinear susceptibility $\chi^{(3)}$ increases with increasing refractive index[5,6], combination of polyimide with a higher refractive index material could result in even higher third-order nonlinearity. Among the various materials available for refractive index tuning[7], $Ta_2O_5$ is a well-known high refractive index material that exhibits also high third order nonlinearity[8,9] and is transparent over a broad wavelength range 300-8000 nm[10,11]. Moreover, $Ta_2O_5$ is stable under laser radiation[12].

Atomic layer deposition (ALD)[13,14] is an optimal technique to deposit thin films for optics because its unique self-limiting growth mechanism enables accurate thickness control and superior conformality also on large areas and patterned surfaces. The selection of materials available by ALD is wide, and also nanolaminates and other artificial structures can be formed in a well controlled manner. The films are of high quality and pinhole-free.

Only few papers report third-order nonlinear properties of ALD-grown thin films. 500 nm thick $ZnO/Al_2O_3$ nanolaminates deposited by ALD showed enhanced third

harmonic generation as compared to a plain ZnO film with a similar thickness[15,16]. $TiO_2/Al_2O_3$ nanolaminates[16] and $ZnS/Al_2O_3$ mixture films[17] deposited by ALD showed third-order nonlinearities lower than plain $TiO_2$ and ZnS, respectively. In all these, a material with high third order nonlinearity (ZnS, ZnO, or $TiO_2$) was combined with $Al_2O_3$ that does not exhibit high third-order nonlinearity.

We have earlier deposited polyimide/$Ta_2O_5$ nanolaminates in a slot-waveguide ring resonator[18]. Our results showed confinement not only in the central air slot between two nanolaminate-coated rails, but also in the sub-10-nm vertical polyimide slots formed by the nanolaminate structure. Our devices showed high Q factors and low propagation losses, indicating their applicability in silicon nanophotonic devices[18].

In this study we investigated third-order nonlinearity of polyimide/$Ta_2O_5$ nanolaminates deposited by atomic layer deposition. Both polyimide and $Ta_2O_5$ have high third-order nonlinearities, which makes this system different to the nanolaminates studied earlier. The layer thicknesses in the nanolaminates were varied, and third harmonic generation in the nanolaminates was compared to plain polyimide and $Ta_2O_5$ reference films.

## II. EXPERIMENTAL

Polyimide/$Ta_2O_5$ nanolaminates were deposited as in[19] in an F120 ALD reactor (ASM Microchemistry, Ltd.) on 5 cm x 5 cm soda lime glass and Si substrates at 170 °C. The reactor was operated at a pressure of 10 mbar and nitrogen was used as a carrier and purging gas. Precursors for the polyimide were PMDA (1,2,4,5-benzenetetracarboxylic anhydride, pyromellitic anhydride) and DAH (1,6-diaminohexane)[20] (Figure 1) and for

$Ta_2O_5$ $Ta(OEt)_5$ and $H_2O$[21]. PMDA, DAH and $Ta(OEt)_5$ were vaporized at 150°C, 35°C and 90°C, respectively, from glass boats inside the reactor. $H_2O$ was vaporized from an external source at room temperature. Pulse durations were 4 s for PMDA, 3 s for DAH, 2 s for $Ta(OEt)_5$ and 3 s for $H_2O$. All purge durations were 5 s. The polyimide/$Ta_2O_5$ nanolaminate films deposited using these processes are uniform[19]. The target structures of the nanolaminates are presented in Table 1.

PMDA
= 1,2,4,5-Benzenetetracarboxylic anhydride
= Pyromellitic dianhydride

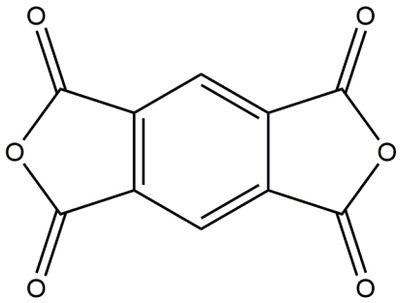

DAH
= 1,6-diaminohexane

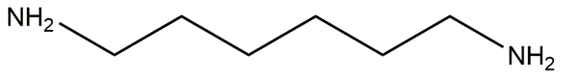


Figure 1. Precursors used for polyimide films.

Thicknesses and refractive indices (at 517 nm) were determined by fitting transmission spectra with a program described in ref. 22 where a one-term Sellmeier equation is used for refractive indices. The spectra were measured with a Hitachi U2000 spectrophotometer at the wavelength range of 370-1100 nm. The nanolaminates were

modelled as single layers. A Hitachi S-4800 field emission scanning electron microscope was used for confirming the nanolaminate structures. EDS measurements were made with an Oxford INCA energy dispersive x-ray spectrometer connected to the Hitachi SEM to estimate the actual amount of $Ta_2O_5$ in the nanolaminates. The $Ta_2O_5$ thicknesses in the nanolaminates were calculated with a GMFILM program[23] from the k ratios measured at 25 keV for the Ta Lα line. The plain $Ta_2O_5$ film was used as a reference.

Multiphoton microscope described in ref. 24 was used for measuring the third harmonic signal. The system has an erbium-doped mode-locked fiber laser as an excitation source. The laser operates at a wavelength of 1.55 μm and it is mode-locked by a carbon nanotube saturable absorber. The maximum average power of the laser was 60 mW with a repetition rate of 50 MHz, pulse duration 150 fs, estimated pulse peak power of 8 kW and a pulse energy of 1.2 nJ.

# III. RESULTS AND DISCUSSION

## *A. Structure and refractive index*

The nanolaminates consisted of 6 bilayers of polyimide + $Ta_2O_5$ and were designed to have a total thicknesses of 120 nm. The first layer of the bilayer was in most cases polyimide, followed by a $Ta_2O_5$ film. The thicknesses of the polyimide and $Ta_2O_5$ layers were varied to see the effect of the changing material content on the optical properties. For comparison, one nanolaminate was prepared with a reversed order of layers (first $Ta_2O_5$, then polyimide) and another one with 12 bilayers instead of 6.

The target structures as well as their measured thicknesses, refractive indices and $Ta_2O_5$ thicknesses are shown in Table 1. It has been observed earlier that the actual layer

thicknesses in nanolaminates may differ from the target values[18,19]. Therefore the refractive indices and nonlinear optical properties are reported here as a function of the measured $Ta_2O_5$ thickness in each nanolaminate. The lowest refractive index (1.58 at 517 nm) was measured for the polyimide reference film and the highest refractive index (2.10 at 517 nm) for the $Ta_2O_5$ film. As expected, the refractive indices of the nanolaminates increased with increasing $Ta_2O_5$ content. This is also seen in Figure 2. From Figure 2 it is also clear that the refractive index does not show a perfectly linear dependence on the measured $Ta_2O_5$ content. Instead, the nanolaminates have lower than expected refractive indices. This is probably due to inaccuracy in the $Ta_2O_5$ thickness measurement by EDS. The relative error is estimated to be about ±10%. UV-vis transmission measurement allows a highly accurate determination of refractive index and film thickness for a single uniform layer of homogeneous material. The simplifying one-layer model employed here probably introduces some error both to the total film thickness and to the refractive index. Despite this, the refractive index dependence is nearly linear over the nominal composition range from 0 to 50 vol.% $Ta_2O_5$ (measured $Ta_2O_5$ thickness 0-62 nm), indicating that the refractive index can be tuned in a straightforward manner over this range.

Table 1. Target structures and measured properties of polyimide/$Ta_2O_5$ nanolaminates

| Target structure | Nominal $Ta_2O_5$ content [vol.%] | Thickness [nm] | n (517 nm) | Measured $Ta_2O_5$ thickness [nm] |
|---|---|---|---|---|
| Polyimide reference | 0 | 121 | 1.58 | 0 |

| | | | | |
|---|---|---|---|---|
| 6 x [15 nm polyimide + 5 nm $Ta_2O_5$] | 25 | 116 | 1.66 | 25 |
| 6 x [10 nm polyimide + 10 nm $Ta_2O_5$] | 50 | 120 | 1.81 | 62 |
| 6 x [5 nm polyimide + 15 nm $Ta_2O_5$] | 75 | 122 | 1.83 | 81 |
| $Ta_2O_5$ reference | 100 | 120 | 2.10 | 120 |
| | | | | |
| 6 x [10 nm $Ta_2O_5$ + 10 nm polyimide] | 50 | 122 | 1.73 | 52 |
| 12 x [10 nm polyimide + 10 nm $Ta_2O_5$] | 50 | 218 | 1.91 | - |

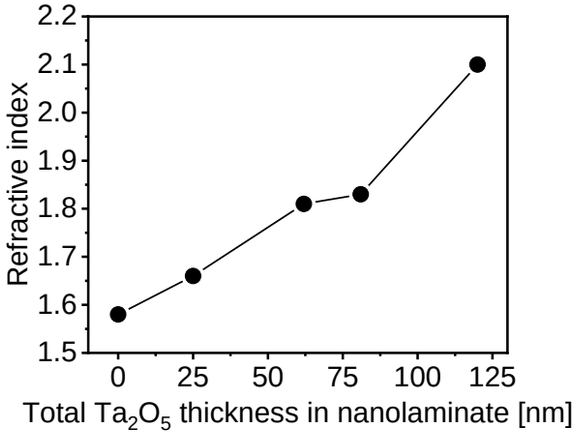


Figure 2. Refractive indices of the nanolaminates and polyimide and $Ta_2O_5$ reference samples at 517 nm as a function of measured $Ta_2O_5$ thickness.

Figure 3 shows a nanolaminate structure with 12 bilayers and confirms clearly that the structure indeed consists of distinct polyimide and $Ta_2O_5$ layers.

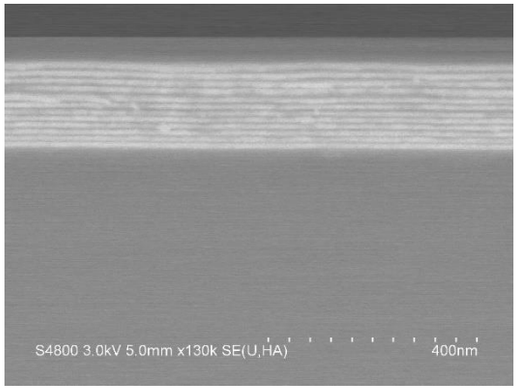


Figure 3. SEM image of a polyimide/$Ta_2O_5$ nanolaminate with 12 bilayers. Dark layers = polyimide, bright layers = $Ta_2O_5$.

## *B. Third-order nonlinearity*

Third order nonlinearities of the polyimide/$Ta_2O_5$ nanolaminates were studied with a multiphoton microscope[24]. The measurements were made similarly as in refs. 15, 16. The laser spot diameter was about 1.8 μm. The THG signal was selected using a 520 ± 10 nm bandpass filter. For each sample, three (3) areas about 1 mm apart from each other were measured. The THG signal was averaged over 512 x 512 points on each rectangular 260 μm x 260 μm measurement area.

All the polyimide/$Ta_2O_5$ nanolaminates as well as plain polyimide and $Ta_2O_5$ films produced a third harmonic signal. The measured third harmonic signals are shown in Figure 4. No second harmonic generation was detected. The highest third harmonic generation was measured for the polyimide reference film and the lowest for the $Ta_2O_5$ reference film.

Among the nanolaminates, the one with nominally 75 vol.% $Ta_2O_5$ (81 nm $Ta_2O_5$) gave the lowest third harmonic signal, and the third harmonic generation seemed to increase slightly with increasing polyimide content. However, the third harmonic values

were very close to each other, and the differences between the different nanolaminates may not be significant. Despite that, the various nanolaminates have clearly different refractive indices as shown above in Table 1 and Figure 2. Thus, the addition of $Ta_2O_5$ in the nanolaminate increases the refractive index while still maintaining the THG at almost constant level, which allows to tune the refractive index and THG independently and thus makes these nanolaminates attractive to use in silicon nanophotonics. The samples with 50-75 vol.% (or 62-81 nm) $Ta_2O_5$ seem to be the optimum because they combine a high THG and a high refractive index.

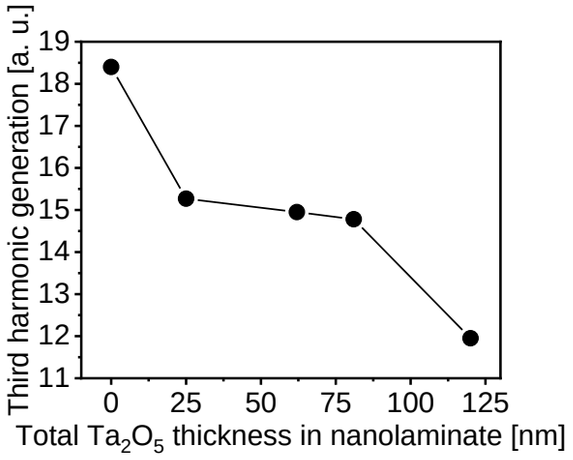


Figure 4. Third harmonic generation in polyimide/$Ta_2O_5$ nanolaminates and polyimide and $Ta_2O_5$ reference samples as a function of measured $Ta_2O_5$ thickness.

Normalized third-order nonlinear susceptibilities, $\chi^{(3)}$, were calculated from the THG values as in refs. 15, 16. Briefly, the THG signal is proportional to the square of $(V\cdot\chi^{(3)})$[15,16]. Taking into account that the illuminated area is equal for all samples, $\chi^{(3)}$ can be calculated if the film thickness is known. Before calculating $\chi^{(3)}$, the measured THG signals were first normalized to the THG signal measured for the plain polyimide film, and the film thicknesses were normalized to the thickness of the plain polyimide film.

The relative error is estimated to be below 10%. The results are shown in Table 2 and Figure 5.

The relative $\chi^{(3)}$ values of the plain polyimide and $Ta_2O_5$ were quite close to each other. This is in agreement with literature. The $\chi^{(3)}$ value for PMDA-DAH has not been reported in the literature, but for PMDA-PDA (PDA = *p*-phenylenediamine) $\chi^{(3)}$ of $7x10^{-13}$ esu at the fundamental wavelength of 1907 nm has been reported[4]. The $\chi^{(3)}$ reported for $Ta_2O_5$ is $2x10^{-13}$ esu at 1550 nm[9]. All the nanolaminate films had lower third-order nonlinear susceptibilities than the plain polyimide. The relative $\chi^{(3)}$ values were so close to each other that the differences between different samples are probably not significant. Also, so there is no enhancement in $\chi^{(3)}$ by the nanolaminate structure. In that sense our results are in agreement with those reported for $TiO_2/Al_2O_3$ nanolaminates[16] and with our earlier observations of $ZnS/Al_2O_3$ mixture films[17] but different from what was observed for $ZnO/Al_2O_3$ nanolaminates[15,16].

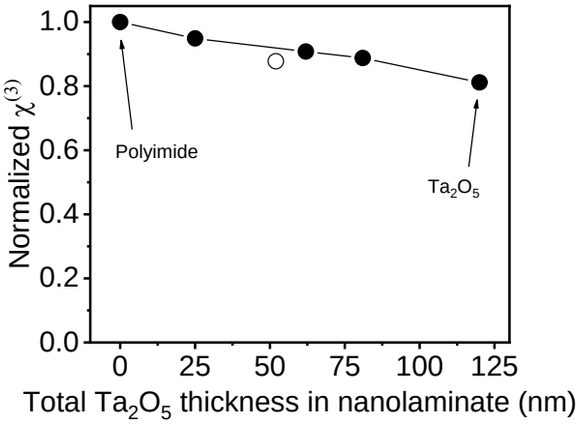


Figure 5. Normalized third-order nonlinear susceptibility, $\chi^{(3)}$, as a function of measured $Ta_2O_5$ thickness. Closed circles = nanolaminates with polyimide as the first layer. Open circle = nanolaminate with $Ta_2O_5$ as the first layer.

We studied also the effect of film thickness on the third harmonic generation. Interestingly, film thickness – at least over the range of our samples – did not seem to affect the third harmonic generation significantly. In the case of polyimide, the third harmonic signals measured for 121 nm and 189 nm thick films were very close to each other. The same was true for $Ta_2O_5$ films when the film thickness was increased by 50 nm. The same effect was seen in the polyimide/$Ta_2O_5$ nanolaminates, too: doubling the nanolaminate target thickness to 240 nm while keeping the thicknesses of polyimide and $Ta_2O_5$ layers at 10 nm did not increase the third harmonic generation. THG signal is enhanced by interfaces[25,26], and thus doubling the number of layers should result in a higher signal. However, in the case of our polyimide/$Ta_2O_5$ nanolaminates this was obviously not the case.

The harmonic signal varies sinusoidally with film thickness, showing maxima at thicknesses corresponding to coherence length and its odd multiples and minima at thicknesses corresponding to its even multiples. Das et al.[27] studied THG in sputtered $TiO_2$ thin films as a function of thickness. The optimum (highest) THG was found in 180 nm thick films, in agreement with the calculated coherence length of 190 nm at the fundamental wavelength of 800 nm[27]. In our case it is obvious that the thicknesses of all films are far below the coherence length. Therefore we expect slow variation in THG signal with the film thicknesses in our experiments. To confirm this, the coherence lengths $L_c$ were calculated from Eq. (1).

$$L_c = \frac{\lambda}{6(n_{517} - n_{1550})} \quad (1)$$

Where λ is the excitation wavelength and $n_{517}$ and $n_{1550}$ are the refractive indices at the excitation wavelength (1550 nm) and at the THG wavelength (517 nm), respectively.

The refractive indices for $Ta_2O_5$ and PMDA-DAH films at 1550 nm were extrapolated from the UV-vis data[22] and were 2.01 and 1.46, respectively. Thus the coherence lengths at 1550 nm were 2.9 μm for $Ta_2O_5$ and 2.2 μm for polyimide.

In contrast to the behavior observed in $Ta_2O_5$, polyimide and their nanolaminates, ALD-grown $Nb_2O_5$ thin films measured for comparison showed increasing third harmonic signal with increasing film thickness (See Figure 6). The $Nb_2O_5$ films were deposited at 200-230°C from $Nb(OEt)_5$ and $H_2O$[28] and their thicknesses were between 112 and 288 nm. Thus the dependence of THG intensity on film thickness seems to be different for different thin film materials. The coherence length for $Nb_2O_5$ was estimated to be the same order of magnitude as for $Ta_2O_5$ and polyimide.

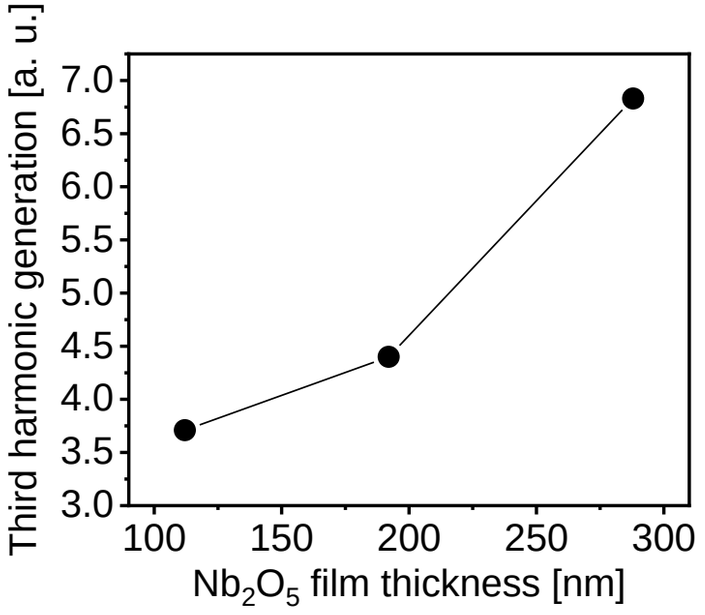


Figure 6. THG measured for ALD-$Nb_2O_5$ films as a function of film thickness.

Table 2. Measured and normalized THG and normalized third-order nonlinear susceptibility for polyimide, $Ta_2O_5$ and nanolaminates.

| Sample | Measured $Ta_2O_5$ thickness [nm] | Measured THG | THG normalized to PI | $\chi^{(3)}$ normalized |
|---|---|---|---|---|
| Polyimide | 0 | 18.44 | 1.00 | 1.00 |
| 6 x [15 polyimide + 5 $Ta_2O_5$] | 25 | 15.27 | 0.83 | 0.95 |
| 6 x [10 polyimide + 10 $Ta_2O_5$] | 62 | 14.95 | 0.81 | 0.91 |
| 6 x [5 polyimide + 15 $Ta_2O_5$] | 81 | 14.78 | 0.80 | 0.89 |
| $Ta_2O_5$ | 120 | 11.95 | 0.65 | 0.81 |
| | | | | |
| 6 x [10 $Ta_2O_5$ + 10 polyimide] | 52 | 14.44 | 0.78 | 0.88 |
| 12 x [10 polyimide + 10 $Ta_2O_5$] | - | 13.24 | 0.72 | 0.47 |

# IV. SUMMARY AND CONCLUSIONS

Third-order optical nonlinearity in ALD-grown polyimide/$Ta_2O_5$ nanolaminates was studied by measuring third harmonic generation with a multiphoton microscope. Various nanolaminates with different layer thicknesses were studied and their third harmonic signals and refractive indices were compared to those measured of polyimide and $Ta_2O_5$ reference films. Both polyimide and $Ta_2O_5$ showed third harmonic generation. Third harmonic generation in the nanolaminates decreased very slightly and refractive index increased with increasing $Ta_2O_5$ content. This makes it possible to fine-tune the refractive index while keeping the third harmonic signal almost constant. Normalized third-order nonlinear susceptibilities, $\chi^{(3)}$, calculated for the nanolaminates were between

the values of $Ta_2O_5$ and polyimide and increased almost linearly with increasing polyimide content.

## ACKNOWLEDGMENTS

The authors thank Dr. Lasse Karvonen and Dr. Antti Säynätjoki for sharing their insight on measuring thin films with multiphoton microscopy and for discussion on the results. The work of the Helsinki group was funded partly by the Academy of Finland (Grant no. 251142 and the Finnish Centre of Excellence in Atomic Layer Deposition). The Arizona group acknowledge support from TRIF Photonics at University of Arizona and NSF CIAN ERC.

[1]M. Borghi, C. Castellan, S. Signorini, A. Trenti, and L. Pavesi, J. Opt. **19**, 093002 (2017).

[2]S. Fathpour, Nanophotonics-Berlin **4**, 143 (2015).

[3]C. Koos, P. Vorreau, T. Vallaitis, P. Dumon, W. Bogaerts, R. Baets, B. Esembeson, I. Biaggio, T. Michinobu, F. Diederich, W. Freude and J. Leuthold, Nat. Photonics **3**, 216 (2009).

[4]S. Morino, T. Yamashita, K. Horie, T.Wada, and H. Sasabe, React. Funct. Polym. **44**, 183 (2000).

[5]H. Tichá, L. Tichý, J. Optoelectron. Adv. Mater. **4**, 381 (2002).

[6]M. Arif, M. Shkir, S. AlFaify, A. Sanger, P. M. Vilarinho, and A. Singh, Opt. Laser Technol. **112**, 539 (2019).

[7]J. Loste, J.-M. Lopez-Cuesta, L. Billon, H. Garay, M. Save, Prog. Polym. Sci. **89**, 133 (2019).

[8]C.-Y. Tai, J. Wilkinson, N. Perney, M. Netti, F. Cattaneo, C. Finlayson, and J. Baumberg, Opt. Express **12**, 5110 (2004).

[9]R. Y. Chen, M. D. B. Charlton, and P. G. Lagoudakis, Opt. Lett. **34**, 1135 (2009).

[10]A. Z. Subramanian, G. S. Murugan, M. N. Zervas, and J. S. Wilkinson, Opt. Commun. **285**, 124 (2012).

[11]M. Belt, M. L. Davenport, J. E. Bowers, and D. J. Blumenthal, Optica **4**, 532 (2017).

[12]J. Jasapara, A. V. V. Nampoothiri, W. Rudolph, D. Ristau, and K. Starke, Phys. Rev. B **63**, 045117 (2001).

[13]V. Miikkulainen, M. Leskelä, M. Ritala, and R. L. Puurunen, J. Appl. Phys. **113**, 021301 (2013).

[14]A. J. M. Mackus, J. R. Schneider, C. MacIsaac, J. G. Baker, and S. F. Bent, Chem. Mater. **31**, 1142 (2019).

[15]L. Karvonen, A. Säynätjoki, Y. Chen, H. Jussila, J. Rönn, M. Ruoho, T. Alasaarela S. Kujala, R. A. Norwood, N. Peyghambarian, K. Kieu, and S. Honkanen, Appl. Phys. Lett. **103**, 031903 (2013).

[16]L. Karvonen, T. Alasaarela, H. Jussila, S. Mehravar, Y. Chen, A. Säynätjoki, R. A. Norwood, N. Peyghambarian, K. Kieu, S. Honkanen, and H. Lipsanen, Proc. SPIE **8982**, 898200 (2014).

[17]E. Färm, M. Kemell et al., manuscript in preparation

[18]A. Autere, L. Karvonen, A. Säynätjoki, M. Roussey, E. Färm, M. Kemell, X. Tu, T.-Y. Liow, G.-Q. Lo, M. Ritala, M. Leskelä, S. Honkanen, H. Lipsanen, and Z. Sun, Opt. Express **23**, 26940 (2015).

[19]L. D. Salmi, E. Puukilainen, M. Vehkamäki, M. Heikkilä, and M. Ritala, Chem. Vapor Depos. **15**, 221 (2009).

[20]M. Putkonen, J. Harjuoja, T. Sajavaara, and L. Niinistö, J. Mater. Chem. **17**, 664 (2007).

[21]K. Kukli, M. Ritala, and M. Leskelä, J. Electrochem. Soc. **142**, 1670 (1995).

[22]M. Ylilammi, and T. Ranta-aho, Thin Solid Films **232**, 56 (1993).

[23]R. A. Waldo, Microbeam Anal. **1988**, 310.

[24]K. Kieu, S. Mehravar, R. Gowda, R. A. Norwood, and N. Peyghambarian, Biomed. Opt. Express **4**, 2187 (2013).

[25]T. Y. F. Tsang, Phys. Rev. A **52**, 4116 (1995).

[26]Y. Barad, H. Eisenberg, M. Horowitz, and Y. Silberberg, Appl. Phys. Lett. **70**, 922 (1997).

[27]S. Kumar Das, C. Schwanke, A. Pfuch, W. Seeber, M. Bock, G. Steinmeyer, T. Elsaesser, and R. Grunwald, Opt. Express **19**, 16985 (2011).

[28]K. Kukli, M. Ritala, M. Leskelä, and R. Lappalainen, Chem. Vapor Depos. **4**, 29 (1998).

## TABLES

Table 2. Target structures and measured properties of polyimide/$Ta_2O_5$ nanolaminates

| Target structure | Nominal $Ta_2O_5$ content [vol.%] | Thickness [nm] | n (517 nm) | Measured $Ta_2O_5$ thickness [nm] |
|---|---|---|---|---|
| Polyimide reference | 0 | 121 | 1.58 | 0 |
| 6 x [15 nm polyimide + 5 nm $Ta_2O_5$] | 25 | 116 | 1.66 | 25 |
| 6 x [10 nm polyimide + 10 nm $Ta_2O_5$] | 50 | 120 | 1.81 | 62 |
| 6 x [5 nm polyimide + 15 nm $Ta_2O_5$] | 75 | 122 | 1.83 | 81 |
| $Ta_2O_5$ reference | 100 | 120 | 2.10 | 120 |
| | | | | |
| 6 x [10 nm $Ta_2O_5$ + 10 nm polyimide] | 50 | 122 | 1.73 | 52 |
| 12 x [10 nm polyimide + 10 nm $Ta_2O_5$] | 50 | 218 | 1.91 | - |

Table 2. Measured and normalized THG and normalized third-order nonlinear susceptibility for polyimide, $Ta_2O_5$ and nanolaminates.

| Sample | Measured $Ta_2O_5$ thickness [nm] | Measured THG | THG normalized to PI | $\chi^{(3)}$ normalized |
|---|---|---|---|---|
| Polyimide | 0 | 18.44 | 1.00 | 1.00 |
| 6 x [15 polyimide + 5 $Ta_2O_5$] | 25 | 15.27 | 0.83 | 0.95 |
| 6 x [10 polyimide + 10 $Ta_2O_5$] | 62 | 14.95 | 0.81 | 0.91 |
| 6 x [5 polyimide + 15 $Ta_2O_5$] | 81 | 14.78 | 0.80 | 0.89 |
| $Ta_2O_5$ | 120 | 11.95 | 0.65 | 0.81 |
| | | | | |
| 6 x [10 $Ta_2O_5$ + 10 polyimide] | 52 | 14.44 | 0.78 | 0.88 |
| 12 x [10 polyimide + 10 $Ta_2O_5$] | - | 13.24 | 0.72 | 0.47 |

FIGURE CAPTIONS

Figure 2. Precursors used for polyimide films.

Figure 2. Refractive indices of the nanolaminates and polyimide and $Ta_2O_5$ reference samples at 517 nm as a function of measured $Ta_2O_5$ thickness.

Figure 3. SEM image of a polyimide/$Ta_2O_5$ nanolaminate with 12 bilayers. Dark layers = polyimide, bright layers = $Ta_2O_5$.

Figure 4. Third harmonic generation in polyimide/$Ta_2O_5$ nanolaminates and polyimide and $Ta_2O_5$ reference samples as a function of measured $Ta_2O_5$ thickness.

Figure 5. Normalized third-order nonlinear susceptibility, $\chi^{(3)}$, as a function of measured $Ta_2O_5$ thickness. Closed circles = nanolaminates with polyimide as the first layer. Open circle = nanolaminate with $Ta_2O_5$ as the first layer.

Figure 6. THG measured for ALD-$Nb_2O_5$ films as a function of film thickness.

Journal of Vacuum Science Technology A





PMDA
= 1,2,4,5-Benzenetetracarboxylic anhydride
= Pyromellitic dianhydride



DAH
= 1,6-diaminohexane

Journal of Vacuum Science Technology A


PLEASE CITE THIS ARTICLE AS DOI: 10.1116/1.5121589

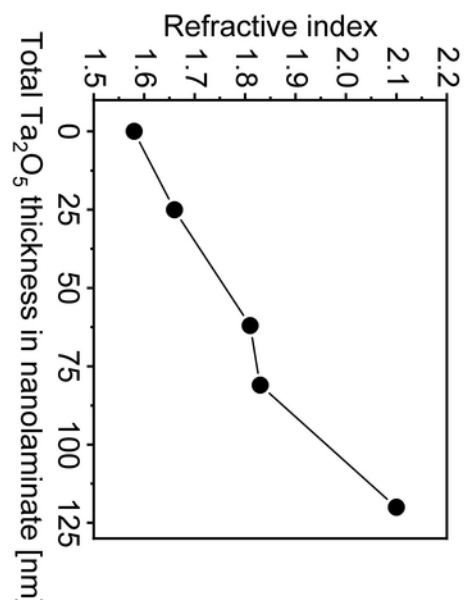

Journal of Vacuum Science Technology A


PLEASE CITE THIS ARTICLE AS DOI: 10.1116/1.5121589

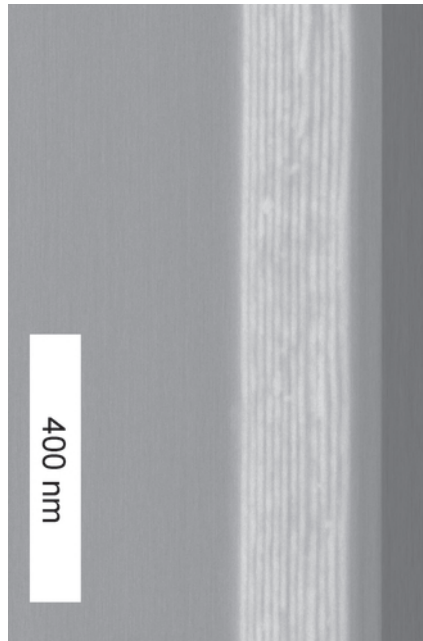

Journal of Vacuum Science Technology A


PLEASE CITE THIS ARTICLE AS DOI: 10.1116/1.5121589

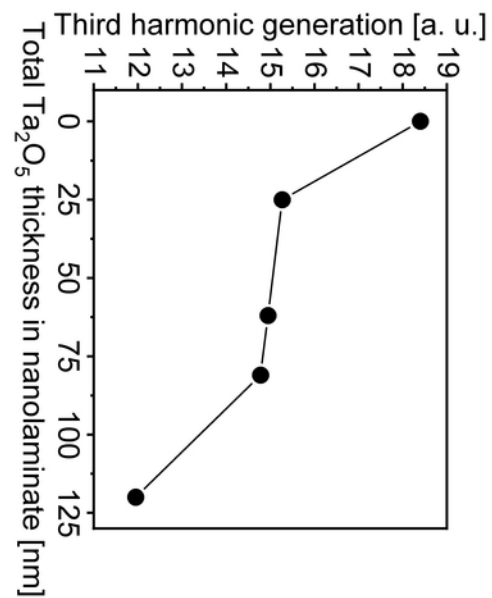

Journal of Vacuum Science Technology A


PLEASE CITE THIS ARTICLE AS DOI: 10.1116/1.5121589

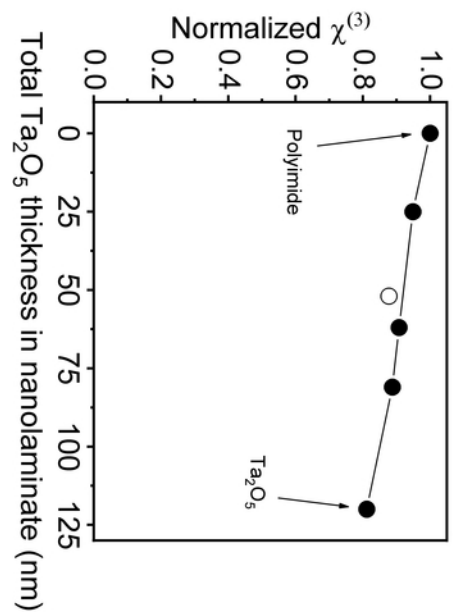

Journal of Vacuum Science Technology A


PLEASE CITE THIS ARTICLE AS DOI: 10.1116/1.5121589